Adv. Radio Sci., 15, 149–155, 2017
https://doi.org/10.5194/ars-15-149-2017

Advances in Radio Science
Open Access Proceedings

Fully integrated high quality factor G_mC bandpass filter stage with highly linear operational transconductance amplifier

Jochen Briem[1], **Marco Mader**[1], **Daniel Reiter**[1], **Raul Amirpour**[1,a], **Markus Grözing**[1], **and Manfred Berroth**[1]

[1]University of Stuttgart, Institute of Electrical and Optical Communications Engineering (INT), Stuttgart, Germany
[a]now at: Fraunhofer-Institut für Angewandte Festkörperphysik (IAF), Freiburg, Germany

Correspondence to: Jochen Briem (jochen.briem@int.uni-stuttgart.de)

Received: 2 January 2017 – Revised: 30 May 2017 – Accepted: 10 June 2017 – Published: 21 September 2017

Abstract. This paper presents an electrical, fully integrated, high quality (Q) factor G_mC bandpass filter (BPF) stage for a wireless 27 MHz direct conversion receiver for a bendable sensor system-in-foil (Briem et al., 2016). The core of the BPF with a Q factor of more than 200 is an operational transconductance amplifier (OTA) with a high linearity at an input range of up to 300 $mV_{pp,diff}$. The OTA's signal-to-noise-and-distortion-ratio (SNDR) of more than 80 dB in the mentioned range is achieved by stabilizing its transconductance G_m with a respective feedback loop and a source degeneration resistors R_{DG}.

The filter stage can be tuned and is tolerant to global and local process variations due to offset and common-mode feedback (CMFB) control circuits. The results are determined by periodic steady state (PSS) simulations at more than 200 global and local process variation parameter and temperature points and corner simulations. It is expected, that the parasitic elements of the layout have no significant influence on the filter behaviour. The current consumption of the whole filter stage is less than 600 µA.

1 Introduction

1.1 Motivation

For the realization of a mechanical flexible sensor system-in-foil all rigid components, like crystal oscillators as frequency reference, have to be avoided. Therefore, a direct conversion receiver for the 27 MHz ISM band is realized, where a high-Q BPF is used for band selection to diminish interferences. To keep the foil system simple and flexible, an integrated on-chip BPF is desired. As inductors for lower frequencies are quite large, and Q factors of on-chip inductors are very limited, they are replaced by active components. Since resistors also use a large area on the chip and no clock reference is available, neither RC filters nor switched-capacitor circuits can be used. Therefore, the BPF is realized by a G_mC circuit, which only consists of OTAs with the transconductance G_m and capacitors with the capacitance C, and can be well integrated in common CMOS technologies (Wangenheim, 2008; Schaumann et al., 1990).

1.2 Filter requirements

For the band selection of the 27 MHz direct conversion receiver, neighbouring bands at 26 and 28 MHz with possibly comparatively high radiated power values of several hundreds of Watts, and other less powerful transmitters in between, should be filtered out. Therefore, an attenuation of at least 30 dB at 0.5 MHz offset and of 50 dB at 1 MHz offset, as well as a maximum ripple of 1 dB in the pass band, are the specified filter characteristics.

A survey of different filter topologies shows that a Butterworth filter with 3 different stages gives the best compromise between circuit requirements and filter characteristics for the mentioned specifications. For this BPF, two stages with a respective Q factor of around 200, and one stage with a Q factor of around 100, are chosen.

2 G_mC circuits

2.1 Basic G_mC circuits

To realize a BPF, different basic functions in G_mC technique are needed. Figure 1 shows the used basic G_mC cir-

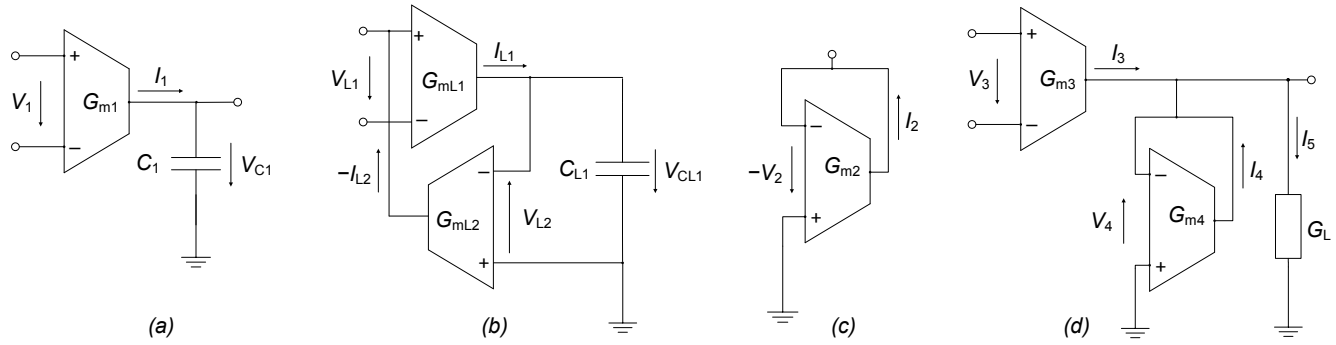

Figure 1. Basic G_mC circuits: **(a)** integrator; **(b)** emulated inductor; **(c)** negative conductance; **(d)** voltage amplifier.

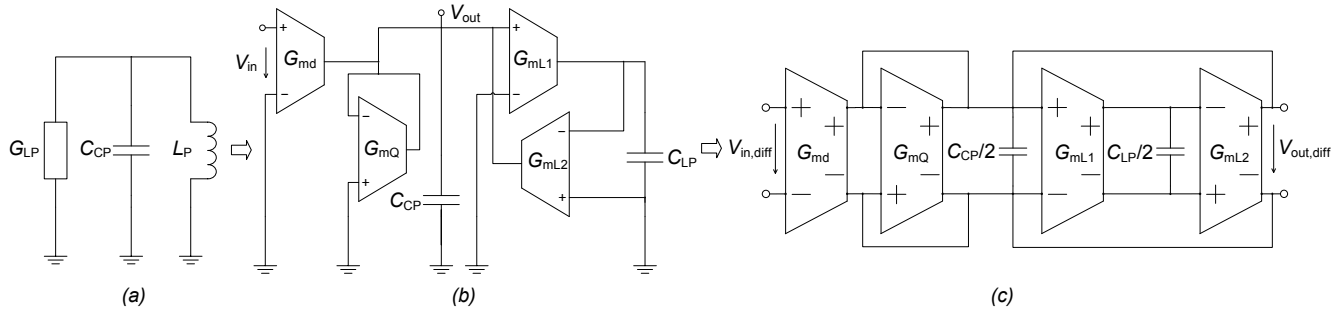

Figure 2. **(a)** *RLC* resonator; **(b)** emulated resonator in G_mC technique and decoupling OTA; **(c)** same as **(b)** but fully differential.

cuits which are an integrator, an emulated inductor, a negative conductance and a voltage amplifier.

The transfer function of the integration shown in Fig. 1a is derived in Eq. (1) (Amirpour, 2015):

$$\frac{V_{\text{out}}}{V_{\text{in}}} = \frac{V_{\text{C1}}}{V_1} = \frac{I_1/\text{j}\omega C_1}{I_1/G_{\text{m1}}} = \frac{G_{\text{m1}}}{\text{j}\omega C_1}. \tag{1}$$

Extending the integrator circuit by a feedback OTA, the behaviour of an inductor can be emulated by two OTAs, which work as a gyrator, and a capacitor. Since phases of currents and voltages are interchanged at inductors and capacitors, the inductor can be emulated as a capacitor, where voltages and currents are interchanged at the in- and output. Figure 1b shows the respective circuit and Eq. (2) proves the proportional behaviour of the reactance versus the frequency and derives the value of the emulated inductor:

$$Z_{\text{in}} = \frac{V_{\text{in}}}{I_{\text{in}}} = \frac{V_{\text{L1}}}{-I_{\text{L2}}} = \frac{V_{\text{L1}}}{-V_{\text{L2}}G_{\text{mL2}}} = \frac{1}{\frac{V_{\text{CL1}}}{V_{\text{L1}}}G_{\text{mL2}}}$$
$$\overset{\text{Eq.(1)}}{=} \frac{\text{j}\omega C_{\text{L1}}}{G_{\text{mL1}}G_{\text{mL2}}} \Rightarrow L = \frac{C_{\text{L1}}}{G_{\text{mL1}}G_{\text{mL2}}}. \tag{2}$$

Figure 1c shows the negative conductance. It is negative, since the differential input voltages are interchanged. Figure 1d depicts the voltage amplifier, which is described by Eq. (3). An additional load conductance G_{L} at the output changes the voltage amplification value.

$$\frac{V_{\text{out}}}{V_{\text{in}}} = \frac{-V_4}{V_3} = \frac{-I_4/G_{\text{m4}}}{V_3} = \frac{I_3 - I_5}{G_{\text{m4}}V_3} = \frac{G_{\text{m3}}}{G_{\text{m4}}} - \frac{V_{\text{out}}G_{\text{L}}}{V_{\text{in}}G_{\text{m4}}}$$
$$\Rightarrow \frac{V_{\text{out}}}{V_{\text{in}}}\left(1 + \frac{G_{\text{L}}}{G_{\text{m4}}}\right) = \frac{G_{\text{m3}}}{G_{\text{m4}}} \Rightarrow \frac{V_{\text{out}}}{V_{\text{in}}} = \frac{G_{\text{m3}}}{G_{\text{m4}} + G_{\text{L}}} \tag{3}$$

2.2 G_mC bandpass filter (BPF) stage

With the basic G_mC circuits, a G_mC BPF stage can be realized with 4 OTAs and two capacitors. The BPF consists of an emulated lossy *LC* resonator with an added negative conductance $-G_{\text{mQ}}$ to compensate for the sum of the losses of the OTAs' output resistances and capacitors through the parallel conductance $G_{\text{LP,OTA}}$. The Q factor can be adjusted through the value of G_{mQ}. To decouple the different filter stages, another OTA is used between the stages with the transconductance G_{md}. Figure 2 shows a conventional *RLC* circuit (Fig. 2a), the respective G_mC equivalent with decoupling (Fig. 2b) and the corresponding fully differential circuit (Fig. 2c). Since the resonant circuit is tuned to resonance at the desired frequency, the load can be described as a real conductor. The decoupling OTA and the Q factor OTA form a voltage amplifier, with the amplification determined according Eq. (3) as the ratio between G_{md} and $G_{\text{mQ}} + G_{\text{L}}$. To minimize the dynamic range requirements of the OTAs, the voltage gain should ideally equal one. Therefore, the values of C_{CP}, C_{LP} and the transconductances should be chosen

in a way, that the voltage swing is similar at all nodes. Additionally, the OTAs should be identical or similar, to reduce the development effort. To realize a small G_{mQ}, two similar transconductors are used in parallel, which are partly cancelling each other. For a better performance, a fully differential circuit is used. The resulting structure can be seen in Fig. 2c.

The resulting centre frequency and Q factor of the BPF stage shown in Fig. 2 is noted in Eq. (4):

$$f_0 = \frac{1}{2\pi\sqrt{C_{CP}L_P}} \overset{\text{Eq.(2)}}{=} \frac{1}{2\pi}\sqrt{\frac{G_{mL1}G_{mL2}}{C_{CP}C_{LP}}};\ Q = \frac{1}{G_{LP}}\sqrt{\frac{C_{CP}}{L_P}}$$
$$= \frac{1}{\left(G_{LP,OTA} - G_{mQ}\right)}\sqrt{\frac{C_{CP}G_{mL1}G_{mL2}}{C_{LP}}} \text{ with } Q = \frac{f_0}{f_{BW}}. \quad (4)$$

3 Operational transconductance amplifier (OTA)

3.1 Requirements

The central part of the G_mC BPF are the OTAs. To achieve a constant centre frequency f_0 and Q factor over the desired dynamic range, very linear OTAs are required. As f_0 is more critical, we first define the maximum allowed deviation of f_0 in respect to the filter bandwidth f_{BW} as $e_{c,max} = \Delta f_0 / f_{BW}$ to determine the OTA's required linearity. Then, Eq. (5) gives the condition for the maximum variation of the transconductance $\Delta G_{mLx,max}$ which depends on the Q factor (Mader, 2016):

$$\frac{1}{2\pi}\sqrt{\left(1 \pm \frac{\Delta G_{mL1}}{G_{mL1}}\right)\left(1 \pm \frac{\Delta G_{mL2,max}}{G_{mL2,max}}\right)\frac{G_{mL1}}{C_{CP}}\frac{G_{mL2}}{C_{LP}}}$$
$$= \frac{1}{2\pi}\sqrt{\frac{G_{mL1}G_{mL2}}{C_{CP}C_{LP}}} \pm e_{c,max}\frac{f_0}{Q} \quad (5a)$$
$$\Rightarrow \sqrt{\left(1 \pm \frac{\Delta G_{mL1,max}}{G_{mL1}}\right)\left(1 \pm \frac{\Delta G_{mL2,max}}{G_{mL2}}\right)}$$
$$= 1 \pm \frac{e_{c,max}}{Q}. \quad (5b)$$

If we assume the same relative variance of the different OTAs, we get the result in Eq. (6):

$$1 \pm \frac{\Delta G_{mL1,2,max}}{G_{mL1,2}} = 1 \pm \frac{e_{c,max}}{Q} \Rightarrow \frac{\Delta G_{mL1,2,max}}{G_{mL1,2}} = \frac{e_{c,max}}{Q}. \quad (6)$$

If we choose $e_{c,max}$ to 0.1, for a Q factor of around 200 a maximum non-linearity of around 0.5 ‰ or around −66 dB is required.

The OTA should keep the linearity requirements in a dynamic range of single-ended peak-to-peak input voltages up to 150 $mV_{pp,se}$.

3.2 Circuit implementation

Like most analogue circuits, the OTA is based on a differential amplifier. Different techniques like cross-coupled amplifiers or current feedback can be used to linearize differential amplifiers. At cross-coupled amplifiers, two different amplifiers are placed in parallel and designed in such a way, that the third harmonics cancel each other, but the first harmonic is not limited too much. This is an energy-efficient way for a linearization and can be realized by different transistor currents and widths, but is strongly dependent on process variations and therefore not used in the realized OTA. Current feedback can be realized by a source degeneration resistor R_{DG}, and leads with a large resistance value R_{DG} to an acceptable linearity despite process variations. The large resistance value can be realized by either resistors or MOSFETs. Because of the limited supply voltages and the relatively large desired dynamic range, the transconductance G_m will be limited in all cases.

To achieve the desired linearity values in the developed OTA, a source degeneration linearization technique is used together with a feedback structure, which additionally keeps the voltage V_{GS} more stable. Therefore, the g_m of the differential switching transistors stays also more stable and hence the amplifier's linearity is further improved. Figure 3 shows a similar basic principle (left panel) and the schematic of the used OTA (right panel). For a high linearity and low process variation dependence, the degeneration is realized by the resistor R_{DG} and not a MOSFET. Together with the transistors N_3 and N_4, the resistor R_{DG} forms the amplifier's core. In Fig. 3 (left panel) the input voltage is transferred to R_{DG} by the feedback loop. The same happens in Fig. 3 (right panel), although the feedback amplifiers have a different input impedance to be realized in a novel, more compact and power efficient way. The gate-source voltage V_{GS} and therefore the g_m of the transistors N_3 and N_4 are also kept more stable by the feedback loop. For example, if V_{in+} is increased, the gate potential of P_1 is decreased and the gate potential of N_3 increased. Consequently, the voltage over R_{DG} and common source voltage of N_1 and N_3 increases. If it increased too much, the feedback loop would decrease it again. Hence the feedback loop stabilizes the voltage over R_{DG} and V_{GS} of N_3. Since the amplifier's output resistance leads to distortions and additionally decreases the quality factor, high output resistances are needed. Thus, cascode current sources (P_5 to P_8) and thick oxid transistors (N_9 and N_{10}) are used at the output path. Cascode current mirrors also enhance the function of the feedback controller (N_5 to N_8). Different supply voltages are needed to keep the transistors in the proper operation region and realize the desired dynamic range. The typical supply voltage of the used 130 nm CMOS technology is 1.2 V. Additionally, supply voltages of $V_{DD1} = 1.8$ V and $V_{DD2} = 2.5$ V are used. Since the voltage is split up between the different transistors, the use of a higher voltage is not critical here. Therefore, at no transistor a voltage of more

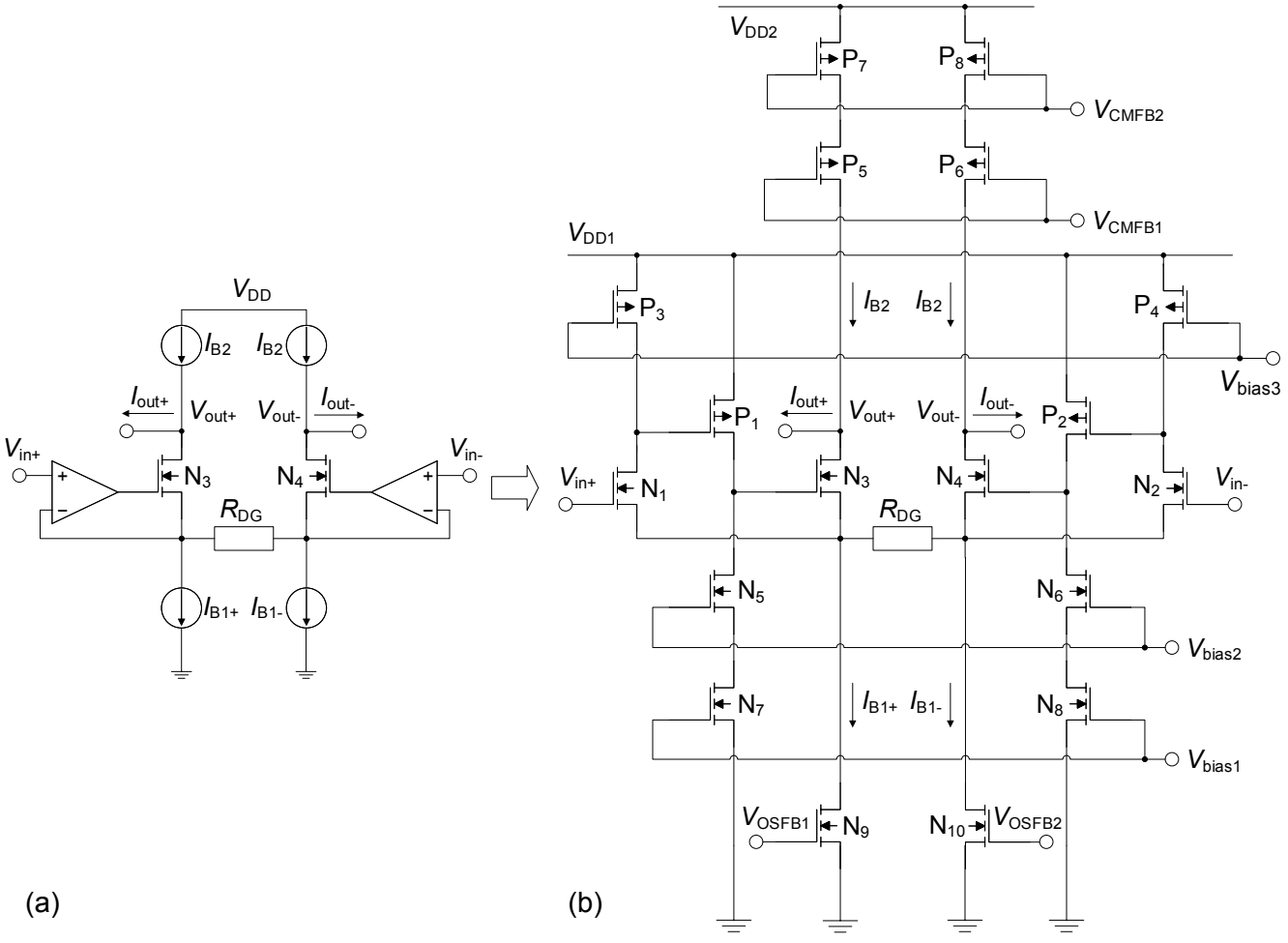

Figure 3. (a) Similar basic concept and **(b)** schematic of the used OTA in the BFP stage.

than 1.2 V is applied. A proper ramp up of the supply voltage prevents the destruction of the transistors at power up.

To keep the output common mode voltage constant, a CMFB control is added, which controls the upper output impedance by V_{CMFB1} and V_{CMFB2} of P_5 to P_8. The output has a simulated standard deviation of 13.3 mV and ensures a proper operation with global and local process variations.

Since local process variations significantly deteriorate the OTA's linearity, an offset feedback (OSFB) control circuit is required. It consists of a differential pair with a negative feedback via V_{OSFB1} and V_{OSFB2} at N_9 and N_{10}. A large time constant is used in the controller so that the influence on the RF-signal is strongly mitigated. For the realization of a simulated standard variation of approx. 4.5 mV and maximum deviation of approx. 12 mV, a high gain and consequently a controller circuit with two stages is used. To tune the OTA's transconductance to the required value after processing, a digital tuning network is added. In it, the value of R_{DG} can be switched in a binary way in the required region.

3.3 Results

Results of DC and PSS simulations of the OTA, all done with the simulator spectre of the design environment cadence, are shown in Fig. 4. In Fig. 4 (left panel), the OTA's differential G_m at DC over the input voltage at an operating point of 1.2 V can be seen. As mentioned earlier, the linear region increases with decreasing transconductance and increasing resistance R_{DG}. In the used OTA, a standard value of around 100 µS is used. Figure 4 (right panel) shows the amplitude spectrum of the periodic differential output voltage with a capacitive load equivalent to the filter circuit with a 27 MHz input voltage of around 300 $mV_{pp,diff}$. The respective SFDR is approx. 85 dBc. It can be seen, that the linearity in the respective input voltage range is higher than required, which further improves the filter stage behaviour.

The current consumption of one complete OTA is around 119 µA, whereof 90 µA are consumed by the OTA itself, 20 µA by the CMFB and around 9 µA by the OSFB.

Table 1 gives a comparison between different OTAs and this work. It can be seen, that the OTA in this work has a high

Table 1. Comparison of the developed OTA.

Publication	CSI 2008	JSSC 2009	APCCAS 2012	This work
Reference	Calvo et al. (2008)	Lo et al. (2009)	Kuo et al. (2012)	
Process (µm)	0.35	0.18	0.18	0.13
Supply voltage (V)	1.8	1.2	1.2	2.5
THD	−58 dB 0.66 Vpp @ 10 MHz	−54 dB 0.6 Vpp @ 20 MHz	−74 dB 0.6 Vpp @ 20 MHz	−80 dB 0.3 Vpp @ 27 MHz
Linear input range (V)	1	1	1	1
Gm (µS)	630–1310	2–110	1–155	50–150
Power (mW)	1.1	1.58	1.9	0.3
Type	measurement	measurement	measurement	simulation with local and global process variation and layout consideration

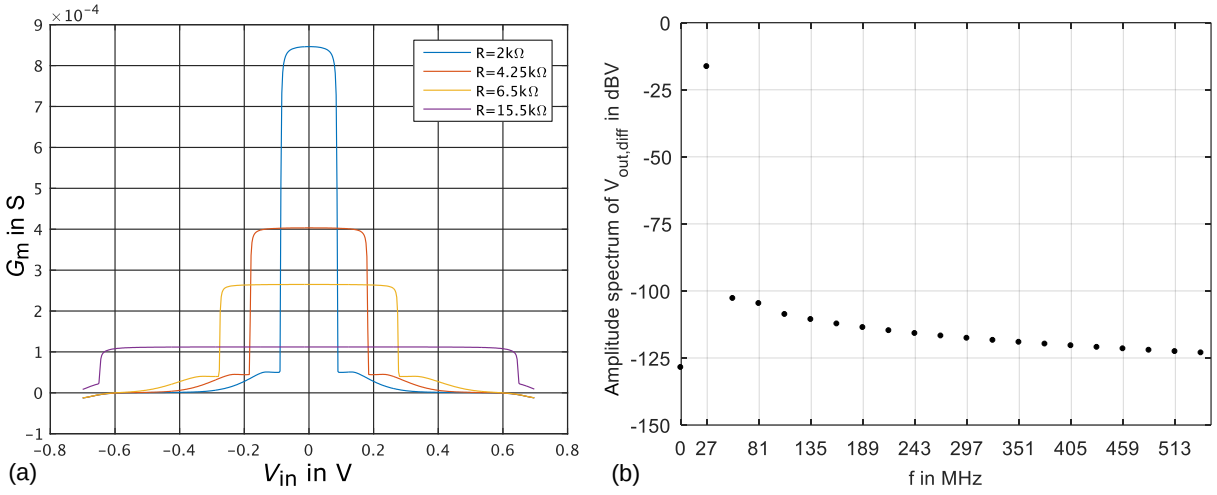

Figure 4. (a) DC simulation with G_m vs. the input voltage V_{in} for different resistor values R_{DG} (Mader, 2016); **(b)** differential output amplitude spectrum at nominal corners for a 27 MHz input with approx. 300 $mV_{pp,diff}$, determined with a PSS simulation (Reiter, 2016).

linearity and a much lower power consumption. The high linearity is critical for the given application.

4 Filter stage results

To determine the performance of the whole filter stage circuit considering global and local process variations in a widespread parameter range, corner simulations of the main devices and Monte Carlo (MC) simulations with 200 runs and latin-hybercube option for all devices are performed. In Fig. 5 (left panel) the time domain signal of the input and output voltages can be seen. Since the voltages are in-phase, the filter stage is tuned to 27 MHz. In Fig. 5 (middle panel), the magnitudes of the filter stage's transfer function are shown for corner simulations of the mainly used transistors with correction of the tuning network. In Fig. 5 (right panel), the same is depicted for the largest deviations of the 200 latin hybercube MC runs without and with correction. The corrected transfer functions almost equal the nominal one. The remaining deviations in maximum magnitude, centre frequency and Q factor can be tolerated, as they are not critical to the filter stage's behaviour.

Simulations with extracted RCC parasitics from the OTA's mask layout show, that there is hardly any effect on behaviour at the desired frequency. Since the filter consists of many interconnected OTAs with capacitive loads of more than 500 fF at each port, the value of additional capacitive parasitics arising from the filter wiring can simply be subtracted from the capacitor values. Therefore, layout parasitics have hardly any effect on the filter behaviour at the desired frequency. The current consumption of one filter stage which consists of five OTAs, each including a CMFB and OSFB, is less than 600 µA.

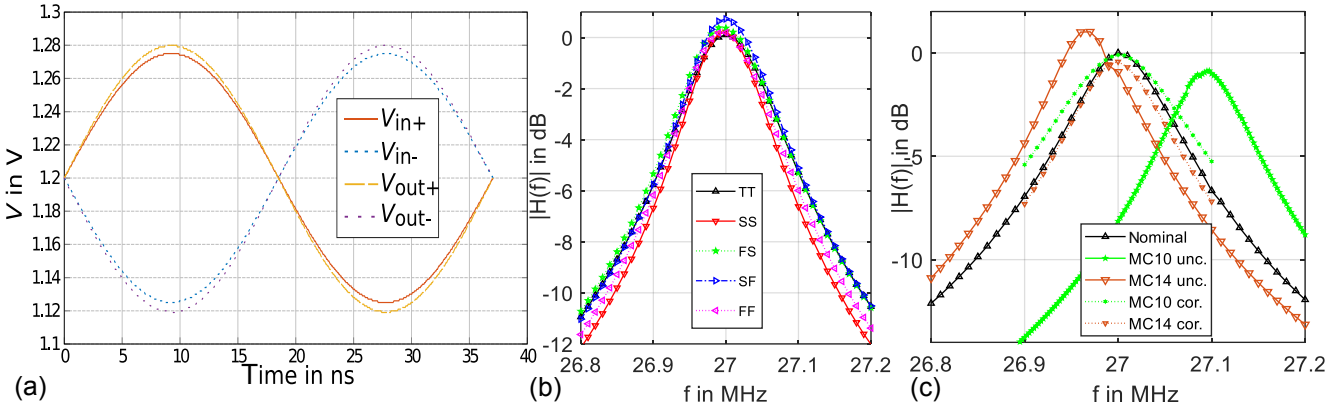

Figure 5. (a) In-phase differential input and output voltages V_{in}, V_{out} of the filter with 27 MHz (PSS simulation) (Mader, 2016); **(b)** magnitude of PSS simulated transfer function for corners of mainly used devices (corrected by tuning network); **(c)** magnitude of PSS simulated transfer function of the filter for largest deviations from the 200 MC latin hybercube simulations without (solid, ∧, *) and with tuning (dotted, smaller ∧, *) (Reiter, 2016).

5 Conclusion

For a direct conversion receiver of a sensor system-in-foil, a fully integrated, active BPF filter stage with a Q factor of more than 200 is developed. It is simulated as a fully differential G_mC design in a 130 nm CMOS technology. Therefore an OTA with a novel feedback concept and a resulting SFDR of more than 82 dB over an input range of 300 $mV_{pp,diff}$ is developed, in order to keep centre frequency and quality factor constant despite varying input levels. To maintain the functionality despite local and global process variations, a CMFB, OSFB and a digital G_m tuning network are used. The results are validated by MC PSS simulations with latin hybercube and 200 runs and corner simulations of the main devices. Resulting from simulations with the OTA's extracted parasitics, no significant chance is expected for the filter behaviour after layout. The current consumption of the whole filter stage is less than 600 µA. In comparison with other OTAs, the developed one has a superior linearity and lower power consumption.

Data availability. Data sets are available in the Supplement.

The Supplement related to this article is available online at https://doi.org/10.5194/ars-15-149-2017-supplement.

Competing interests. The authors declare that they have no conflict of interest.

Acknowledgements. This work was supported by the German BMBF through the KoSiF-Project with grant-no. 1612000508.

Edited by: Jens Anders
Reviewed by: Friedel Gerfers and one anonymous referee

References

Amirpour, R.: Development of an Active GmC Bandpass Filter for a 27 MHz Direct Conversion Receiver in a 500 nm CMOS Gate Array. Study Thesis, Institute of Electrical and Optical Communications Engineering, University of Stuttgart, Stuttgart, 2015.

Briem, J., Grözing, M., and Berroth, M.: A DC-coupled 27 MHz LNA and automatic gain control amplifier on an ultra-Thin 0.5 µm CMOS gate array for a wireless sensor system-in-foil, in: 2016 12th Conference on Ph.D. Research in Microelectronics and Electronics (PRIME), Lisbon, 1–4, https://doi.org/10.1109/PRIME.2016.7519531, 2016.

Calvo, B., Celma, S., Sanz, M. T., Alegre, J. P., and Aznar, F.: Low-Voltage Linearly Tunable CMOS Transconductor With Common-Mode Feedforward, IEEE T. Circ. Syst. I, 55, 715–721, https://doi.org/10.1109/TCSI.2008.919746, 2008.

Kuo, K. C., Chen, S. Y., and Tseng, S. M.: High linear transconductor for multiband CMOS receiver, in: 2012 IEEE Asia Pacific Conference on Circuits and Systems (APCCAS), Kaohsiung, 535–538, https://doi.org/10.1109/APCCAS.2012.6419090, 2012.

Lo, T. Y., Hung, C. C., and Ismail, M.: A Wide Tuning Range Gm-C Filter for Multi-Mode CMOS Direct-Conversion Wireless Receivers, IEEE J. Solid-State Circ., 44, 2515–2524, https://doi.org/10.1109/JSSC.2009.2023154, 2009.

Mader, M.: Development of a High Linearity Operational Transconductance Amplifier for a High Quality Bandpass Filter in a 130 nm CMOS Technology. Study Thesis, Institute of Electrical and Optical Communications Engineering, University of Stuttgart, Stuttgart, 2016.

Reiter, D.: Development of an Offset Feedback Control and a Tuning Block for an integrated High-Q Bandpass Filter in a 130 nm CMOS Technology. Study Thesis, Institute of Electrical and

Optical Communications Engineering, University of Stuttgart, Stuttgart, 2016.

Schaumann, R., Ghausi, M. S., and Laker, K. R.: Design of analog filters: passive, active RC, and switched capacitor, Prentice-Hall, Englewood Cliffs, NJ, 1990.

Wangenheim, L.: Aktive Filter und Oszillatoren: Entwurf und Schaltungstechnik mit integrierten Bausteinen, Springer, Berlin, Heidelberg, https://doi.org/10.1007/978-3-540-71739-3, 2008.